

Contents

1	Scientific, Technical, and Management Section	1
1.1	Baselines and Observables	1
1.2	Science Objectives	1
1.2.1	The Primordial Universe and Cosmic Inflation	1
1.2.2	Light Relics and Dark Matter	4
1.2.3	Neutrino Mass	5
1.2.4	Cosmological structure formation	6
1.3	The Challenges: Foregrounds and Systematics	7
1.3.1	Foregrounds	7
1.3.2	Systematic Errors	9
1.4	Current and Forthcoming Efforts and the CMB Probe	11
1.5	State of Technologies	11
1.6	Mission Study, and Management Plan	14
2	Curriculum Vitae	21
3	Summary of Work Effort	30
4	Current and Pending Support	30
5	Letters of Support	44
6	Budget Details - Narrative	48
6.1	Team, and Work Effort	48
6.1.1	Funded Team Members	48
6.1.2	Non-Funded Team Members	48
6.2	Costing Principles	48
6.3	University of Minnesota Budget	48
6.3.1	Direct Labor	48
6.3.2	Supplies	48
6.3.3	Travel	48
6.3.4	Other Direct Costs	48
6.3.5	Facilities and Administrative Costs	48
7	Budget Sheets	49

1 Scientific, Technical, and Management Section

1.1 Baselines and Observables

We are proposing to study a probe-scale mission to extract the wealth of cosmological information contained in the spectrum and polarization of the cosmic microwave background (CMB). The starting points for our study of this CMB Probe are two current-decade space missions, EPIC-IM and Super-PIXIE [1, 2]. EPIC-IM was presented to the 2010 decadal panel as a candidate CMB imaging polarization space mission. It was based on a 2 m aperture telescope and 11,094 bolometric transition edge sensors. PIXIE is a proposed Explorer-scale mission focused on a measurement of the spectrum and polarization of the CMB on large angular scales. Super-PIXIE is envisioned to be a scaled up, more capable version of PIXIE. It consists of 4 spectrometers, each operating between 30 and 6015 GHz with 400 15 GHz-wide bands. Improvements in technology by the next decade will enable the design of a mission that is more capable compared to EPIC-IM and Super-PIXIE. Therefore, all quantitative predictions presented in this proposal, which are based on EPIC-IM and Super-PIXIE, represent *minimum* capabilities for the CMB Probe.

The best measurements of the CMB spectrum – made by COBE/FIRAS approximately 25 years ago – show that the average CMB spectrum is consistent with that of a blackbody to an accuracy of 4 parts in 10^4 [3, 4]. Distortions in this spectrum encode a wealth of new information. The distortion shapes are commonly denoted as μ - and y -types [5, 6]. The μ -distortion arises from energy release in the early Universe and can only be produced in the hot and dense environment present at high redshifts. This makes μ -distortions a novel messenger from a redshift range $z \geq 5 \times 10^4$. The y distortions are caused by energy exchange between CMB photons and free electrons through inverse Compton scattering. These originate at lower redshifts and are sensitive to the evolution of the large scale structure of the Universe.

Thomson scattering at the surface of last scattering is the source of the polarization of the CMB. It is useful to decompose the polarization field to two modes that are independent over the full sky, E and B modes. Together with the pattern of temperature anisotropy T , the CMB thus gives three auto- and three cross-spectra. The *Planck* satellite and larger aperture ground-based instruments measured the T spectrum to cosmic variance limit for $\ell \leq ??$. Much information remains encoded in the E and B spectra, whose full exploration has just begun [7, 8? ?].

A future CMB Probe-scale mission will address the physics of the big bang and of quantum gravity; it will measure the sum of the neutrino masses, and constrain the effective number of light particle species and the nature of dark matter; it will probe the existence of new forms of matter at the early Universe; it will give new insights on the star-formation history across cosmic times, and it will provide information about the processes that control structure formation. In addressing these broad array of fundamental questions the Probe firmly fits into NASA’s strategic plan as articulated by its Strategic Goal 1 “Expand the frontiers of knowledge”, and specifically Objective 1.6 “Discover how the Universe works, [and] explore how it began and evolved”.

1.2 Science Objectives

1.2.1 The Primordial Universe and Cosmic Inflation

The observed temperature and E -mode polarization of the CMB require primordial inhomogeneities in the gravitational potential, providing a remarkable observational link to the dynamics of the Universe near the big bang. Inflation, a primordial era of accelerated expansion, provides a compelling dynamical origin for the observed nearly scale-invariant spectrum of the primordial perturbations [9, 10, 11, 12, 13]. But, Inflation also predicts an as yet unobserved spectrum of primordial

gravitational waves sourced directly by quantum fluctuations of the tensor component of the metric. These gravitational waves make a distinct B-mode imprint on the polarization of the CMB. Any detection of B-mode polarization, whether generated by the primordial gravitational waves of Inflation [14, 15] or by any other source of early time vector or tensor perturbations, would reveal completely new information about the primordial era. The results would provide significant constraints and consistency checks for current models or could perhaps even overturn them. A detection would have implications for fundamental physics by providing evidence for a new energy scale near the GUT scale. In the context of Inflation, the relationship is particularly clear: the potential energy V of the inflaton is related to the tensor-to-scalar ratio r at the peak of the spectrum by $V^{1/4} = 3.7 \times 10^{16} r^{1/4}$ GeV.

Figure 1 shows current CMB data, B-modes from vacuum fluctuations of the metric during an Inflationary era for two values of r , as well as forecasts for the determination of the CMB spectra for EPIC-IM. The most recent constraint on the tensor to scalar ratio gives $r < 0.07$ (95%); see Figure 2 [18]. For testing inflation, the largest scales $\ell \leq 10$ are particularly important because they reveal the presence of B mode correlations on scales that were super-horizon at the time of recombination [16], and because the signal is strongest relative to the B-mode from lensing. No sub-orbital platform has yet produced B-mode measurements at $\ell < 80$, and a satellite is by far the most suitable platform to making the all sky observations necessary to reach the lowest modes, $\ell < 20$. In its recent report New Worlds New Horizons (NWNH), the decadal survey committee strongly endorsed searches for the B-mode signal from inflation saying that “The convincing detection of B-mode polarization in the CMB produced in the epoch of reionization would represent a watershed discovery.” [17].

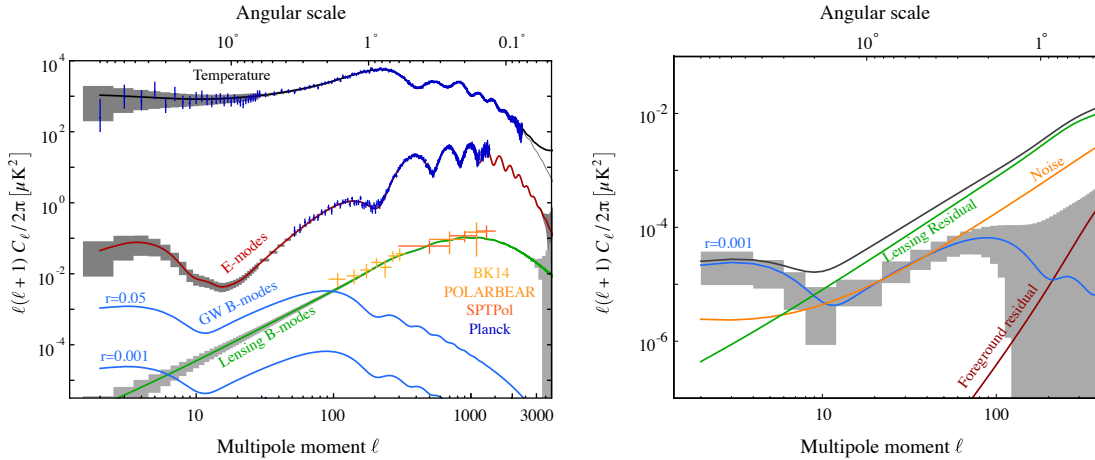


Figure 1: Predicted determination of the CMB power spectra for EPIC-IM (grey boxes) overlaid on theoretical predictions (solid lines) and including Planck measurements of the temperature and E modes (blue) and of several ground-based measurements of the lensing B-modes. The tensor B-mode predictions (blue) are shown for two representative values of the tensor-to-scalar ratio: $r = 0.001$ and $r = 0.05$.

In slow roll Inflation there are just two observationally viable classes of models that naturally explain the measured value of the spectral index n_s . One is the set of potentials $V(\phi) \propto \phi^p$, which contains many of the canonical inflation models. This set is already under significant observational pressure. If the error bars on the spectral index tighten by a factor of about 2, and the 95% C.L. upper limit on r is pushed to even ~ 0.01 , all such models would be ruled out. The other class of models includes Starobinsky and Higgs inflation, which both have $r \sim 0.003$. A future mission capable of reaching $\sigma_r \sim \mathcal{O}(10^{-4})$ would provide significant constraints on nearly every currently

favored inflation model. The EPIC-IM configuration is forecasted to achieve **Raphael will update the following to match figures** $\sigma(r) \sim 4.8 \times 10^{-4}$ assuming $r = 0.01$ and no foregrounds.

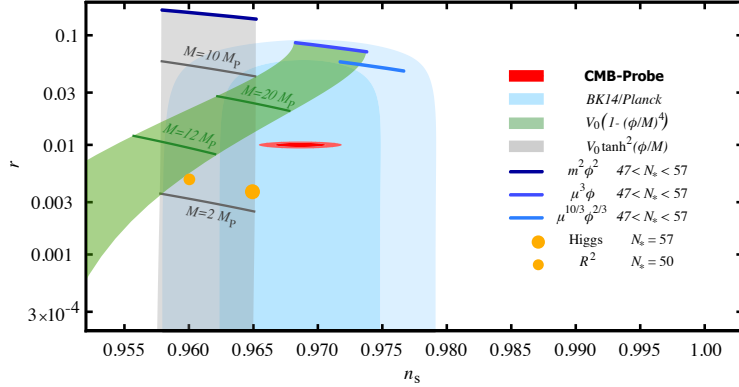


Figure 2: Current 1 and 2σ limits on r and n_s (blue) and forecasted constraints for a fiducial model with $r = 0.01$ for EPIC-IM [18]. Also shown are predictions for the models of the inflaton potential discussed in the text: Chaotic inflation for a range of N_* values (blue lines); Higgs and R^2 (large and small dots, respectively); quartic hilltop (green band); and a sub-class of α -attractor models [19]

A detection of B -modes consistent with a primordial spectrum of vacuum fluctuations would be the first observation of a phenomena directly related to quantum gravity. In addition, any detection with a next generation satellite would be evidence for *large-field* Inflation [20], in which a smooth potential that supports Inflation extends over a distance in field space $\Delta\phi \gtrsim M_p$. Quantum gravity studies of inflation give a generic expectation $\Delta\phi \lesssim M_p$ [21, 22, 23, 24], although there are some mechanisms to realize large-field inflation [25, 26, 27, 28]. A detection of r would therefore provide strong motivation to better understand how large-field inflation can be naturally incorporated into quantum gravity.

All inflation models predict a B -mode spectrum with the shape shown in Figure 1, but inflation need not be correct [29, 30, 31] and does not preclude additional sources of B -mode polarization either during or after inflation. To be confident of the implications of a detection, the shape and Gaussianity of the B -mode spectrum must be characterized. The vast majority of inflation scenarios predict an extremely Gaussian and nearly scale-invariant spectrum for gravitational waves. A target constraint of $\sigma(n_t) < 1$ at $r = 0.01$, driven by the information in the reionization bump, would significantly constrain non-vacuum inflationary sources [32, 33] and rule out physics completely inconsistent with inflation.

Deeper mapping of E -mode polarization will also contribute to testing inflationary models. Large scale E -modes will provide new tests of isotropy, a prediction of most models of Inflation; for example, the observations can reject at 99% confidence models in which low multipoles are aligned in the temperature maps [34]. Together with continued improvements at high ℓ from the ground, these modes will also improve constraints on the scalar spectral index and its changes with scale by factors of about two.

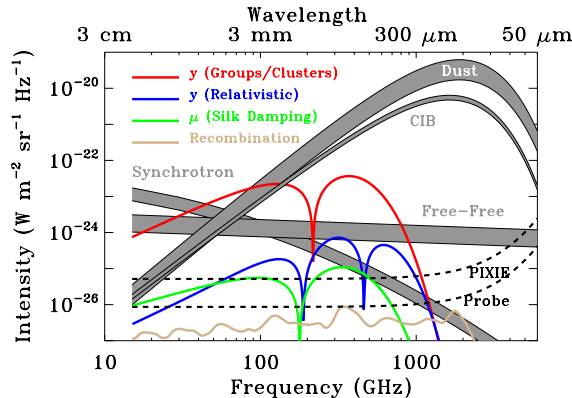


Figure 3: Anticipated y and μ spectral distortions (solid), the signature of resonant recombination lines (solid), and anticipated foreground signal levels relevant for spectral distortion measurements (grey bands). The simplest extension of a proposed Explorer class mission (Probe, dash grey) gives approximately 10 times the Explorer sensitivity (PIXIE). A better optimized Probe may give detections of all anticipated distortions.

Spectral distortion measurements give additional tests of Inflation. The dissipation of small-scale perturbations through Silk-damping leads to μ -distortions [35, 36, 37, 38]. In Λ CDM the distortions are predicted at a level of $\mu = (2.0 \pm 0.14) \times 10^{-8}$, a level that is readily accessible to a Probe class mission, see Fig. 3 [38, 39].

A better optimized probe may also give the sensitivity to detect the signature of recombination radiation imprinted by cosmological recombination of hydrogen and helium at redshift $z \simeq 10^3 - 10^4$; see Fig. 3 [40, 41]. The detailed physics is sensitive to the values of n_s , which is a direct probe of Inflation.

1.2.2 Light Relics and Dark Matter

After inflation, the universe was reheated to temperatures of at least 10 MeV and perhaps as high as 10^{10} GeV. At these high temperatures, even very weakly interacting or very massive particles, such as those arising in extensions of the Standard model of particle physics, can be produced in large abundances [42, 43]. As the universe expands and cools, the particles fall out of equilibrium and leave observable signatures in the CMB power spectra. Through these effects the CMB is a sensitive probe of neutrino and of other particles' properties.

One particularly compelling target is the effective number of light relic particle species N_{eff} , also called the effective number of neutrinos. The canonical value with three neutrino families is $N_{\text{eff}} = 3.046$. Additional light particles contribute a change to N_{eff} of $\Delta N_{\text{eff}} \geq 0.027 g$ where $g \geq 1$ is the number of degrees of freedom of the new particle [44, 45]. This defines a target of $\sigma(N_{\text{eff}}) < 0.027$ for future CMB observations. Either a limit or detection of ΔN_{eff} at this level would provide a powerful insight into the basic constituents of matter.

Forecasts for N_{eff} are shown in Figure 4. The two most important parameters for improving constraints are the fraction of sky observed f_{sky} and the noise. Achieving both larger f_{sky} and lower noise are strengths of the CMB Probe compared to other platforms. Our baseline mission nearly reaches the target constraint with $g = 1$, already exceeding constraints from other astrophysical probes and planned CMB observations. A newly designed mission is likely to reach $\sigma(N_{\text{eff}}) < 0.027$ with high signal-to-noise ratio.

Many light relics of the early universe are not stable. They decay, leaving faint evidence of their past existence on other tracers. The relics with sufficiently long lifetime to survive few minutes, past the epoch of light element synthesis, leave a signature on the helium fraction Y_p . If they decay by the time of recombination, their existence through this period is best measured through the ratio of N_{eff} to Y_p . The Probe's cosmic variance limited determination of the E power spectra will improve current limits for these quantities by a factor of five thus eliminating sub-MeV mass thermal relics. Spectrum distortion measurements give additional constraints on the lifetime and abundance of such relics [47, 48, 49, 50]. A future Probe's μ -distortion constraint gives a two orders of magnitude improvement on the abundance and life time of early Universe relics [51, 52] compared to current constraints derived from measurements of light element abundances [53, 54].

Cosmological measurements have already confirmed the existence of one relic that lies beyond the Standard Model: dark matter. For a conventional WIMP candidate, the CMB places very stringent constraints on its properties through the signature of its annihilation on the T and E spectra [55, 56, 57]. Planck currently excludes WIMPs with mass $m_{\text{dm}} < 16$ GeV and a future CMB mission could reach $m_{\text{dm}} < 45$ GeV for $f_{\text{sky}} = 0.8$. The CMB provides the most stringent constraints on the dark matter annihilation cross section for dark matter in this mass range. The CMB is complimentary to direct detection experiments which probe the scattering cross-section of dark matter with Standard model particles.

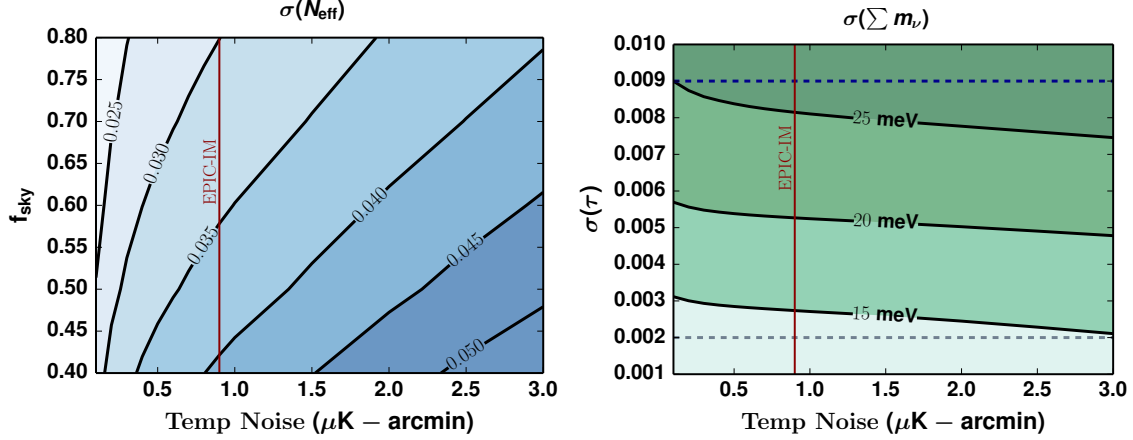


Figure 4: N_{eff} as a function of noise and sky fraction (left) and Neutrino mass constraints as a function of uncertainties in measurement of τ , noise, and sky fraction of $f_{\text{sky}} = 0.7$. The resolution assumed is $5'$. Vertical lines denote the expected performance of EPIC-IM. The blue dashed line is the current *Planck* limit; the grey dashed line is the limit from cosmic variance measurement of τ . All forecasts assume internal delensing of the T and E -maps [46], including residual non-Gaussian covariances. The $\sum m_\nu$ forecasts includes DESI BAO.

A particle-independent approach is to constrain dark matter interactions that would affect the evolution of the effective dark matter fluid and its interactions with baryons or photons. The simplest example is to constrain the baryon-dark matter cross section through its effective coupling of the two fluids [58]. These couplings affect the evolution of fluctuations and ultimately the T and E spectra. The current limits of $\sigma \gtrsim 10^{-31} - 10^{-34} \text{ cm}^2 \times (m_{\text{dm}}/\text{MeV})$ can be competitive with direct detection for sub-GeV masses. More exotic dark sectors that include long-range forces can produce an even richer phenomenology in the CMB and in the large-scale structure without necessarily producing an associated signature in direct detection experiments or indirect searches (e.g. [59, 60, 61]).

Interactions of dark matter with standard model particles can also be constrained through measurements of spectral distortions [62]. Current constraints from FIRAS are most sensitive to small dark matter mass, $m_\chi \lesssim 0.2 \text{ MeV}$, but these could be extended to $m_\chi \lesssim 1 \text{ GeV}$ with a Probe-class mission, testing DM interaction down to cross-sections $\sigma \simeq 10^{-39} - 10^{-35} \text{ cm}^2$ [62]. This provides new constraints on the low mass end, $m_\chi \lesssim 10 \text{ MeV}$ and improve existing limits [63, 64] by up to a factor of $\simeq 50$. Distortion measurements furthermore open a new avenue for testing dark matter-proton interactions [62].

A host of other physical phenomena including the existence and properties of axions, primordial magnetic fields, and superconducting strings, leave signatures on the spectrum of the CMB and can therefore be constrained by the sensitive measurements of a future Probe [e.g., 65, 66, 67, 68, 69].

1.2.3 Neutrino Mass

One of the last unknowns of the Standard model of particle physics is the absolute mass scale of the neutrinos. Cosmology presents a unique opportunity to measure the sum of neutrino masses $\sum m_\nu$ through the suppression of the growth of structures in the Universe on small scales. The sensitivity to $\sum m_\nu$ from suppression of power is limited by our knowledge of the primordial amplitude of fluctuations A_s , which is strongly degenerate with the optical depth τ . The current limit on τ from *Planck* of $\sigma(\tau) = 0.009$ [] limits $\sigma(\sum m_\nu) \gtrsim 25 \text{ meV}$. Forecasts for an internal CMB measurement

of $\sum m_\nu$ via CMB lensing [70] are shown Figure 4 but the conclusion is the same for any proposed cosmological probe. Therefore, a cosmological detection of the minimum value expected from particle physics $\sum m_\nu = 58$ meV at more than 2σ will require a better measurement of τ . The best constraints on τ come from E -modes with $\ell < 20$ which require measurements over the largest angular scales. To date, the only proven method for such a measurement is from space. The CMB Probe will reach the cosmic variance limit of $\tau \sim 0.002$ and will therefore reach $\sigma(\sum m_\nu) < 15$ meV when combined with DESI’s measurements of baryon acoustic oscillations [71]. A detection of $\sum m_\nu$ at this level is not possible with any other existing survey.

1.2.4 Cosmological structure formation

Understanding the evolution of cosmological structures from small density perturbations through the formation of the first stars to present day galaxies and cluster is a key goal of cosmology [72]. Cosmological reionization, the transition of the Universe from dominated by neutral to ionized hydrogen, is a cornerstone of this evolution because it encodes information about the star formation history and the physical processes that formed the galaxies of various luminosities and masses we see today. But when did the epoch of reionization start? How long did it last? Are early galaxies enough to reionize the entire Universe or is another source required?

Measurements of the CMB E mode power spectrum over large angular scales are sensitive to the optical depth to reionization τ , a key parameter for all reionization models that attempt to answer these questions. The *Planck* team reported recently a value of $\tau = 0.055 \pm 0.009$ [? ?]. The level is significantly lower than previous estimates and reduces the tension between CMB-based analyses and constraints from other astrophysical sources. The CMB Probe’s cosmic variance limited measurement of E -mode polarization will improve the 1σ error by a factor of 4.5 to reach a cosmic variance limited measurement of τ , thus setting stringent constraints on models of the reionization epoch.

The anisotropy in the cosmic infrared background (CIB) produced by dusty star-forming galaxies in a wide redshift range, are an excellent probe of both the history of star formation and the link between galaxies and dark matter across cosmic time. The *Planck* collaboration derived values of the star formation rate that, at redshifts $z \sim 3$, are three times larger than constraints from number counts measurements ([73, 74, 75]). The new mission probe, By measuring CIB anisotropy with 100 times higher signal-to-noise ratio the CMB Probe will shed light on this intriguing discrepancy. Specifically, it will constrain the star formation rate with one tenth of *Planck*’s uncertainty.

A key parameter in simulations of the angular power spectrum of the CIB is M_{eff} , the galaxy halo mass that is most efficient in producing star formation activity. Comparing measurements of the power spectrum to simulations constrains this parameter, which informs structure formation models. Current models and measurements find $M_{\text{eff}} \sim 10^{12}$ solar masses with about 10% uncertainty. The CMB Probe will constrain this parameter at the percent level.

The transition to reionized Universe and the onset of structure formation inject energy into the sea of CMB photons. This injection is detectable through a distinct spectral distortion. This is the largest expected distortion – marked ‘ y Groups/Clusters’ in Figure 3 – and will be clearly detected by the CMB Probe. A detection will give information about the total energy output of the first stars, AGNs, and galaxy clusters, an important parameter in structure formation models.

Group-size clusters that have masses $M \simeq 10^{13} M_\odot$ contribute significantly to the signal. With temperature $kT_e \simeq 1$ keV these are sufficiently hot to create a relativistic temperature correction to the large y -distortion. This relativistic correction, denoted ‘ y relativistic’ in Figure 3, will also be detected with high signal-to-noise ratio by the CMB Probe, and will be used to constrain the

currently uncertain feedback mechanisms used in hydrodynamical simulations of cosmic structure formation [76].

The CMB spectrum varies spatially across the sky. One source of such anisotropic distortion is due to the spatial distribution clusters of galaxies and has already been measured by Planck [77]. A combination of precise CMB imaging and spectroscopic measurements will allow observing the relativistic temperature correction of individual SZ clusters [78, 79, 80], which will calibrate cluster scaling relations and inform our knowledge of the dynamical state of the cluster atmosphere.

Resonant scattering of the CMB photons during and post last scattering leads to spectral-spatial signals that can be used to constrain the abundance of metals in the dark ages and therefore the make-up of the first, and subsequent generations of stars [81, 82, 83, 84, 85].

1.3 The Challenges: Foregrounds and Systematics

A minimum target for the CMB Probe is to constrain the tensor-to-scalar ratio with $\sigma(r) < 0.001$. Data from *Planck* and sub-orbital experiments reveal that incomplete knowledge of the polarized foregrounds currently limits the measurements. Reducing r uncertainties from their current $\sim 10^{-1}$ level will have to be accompanied by equivalent higher fidelity measurements of the foregrounds.

A satellite mission provides a unique opportunity to target both the inflationary B -mode polarization that originates from the epoch of recombination and peaks around $\ell = 80$ and the contribution from reionization that peaks on significantly larger scales, $\ell \lesssim 12$. Measuring the latter will require an unprecedented understanding of foregrounds and systematic effects. This is illustrated in the left panel of Figure 5, which shows the contribution from reionization to the Stokes Q parameter for $r = 0.001$; the amplitude of the signal is approximately 10 nK.

The CMB Probe has complete flexibility in the choice of spatial and frequency coverage, both of which are challenging from the ground or from the balloon platform. Among other limitations, the atmosphere prevents observations at key frequencies, such as 60 GHz, and requires data filtering that makes it difficult to recover the larger angular scales.

By the time a probe-class mission launches, substantial progress will have been made in this quest. In the absence of a primordial B -mode signal at detectable levels, the mission will significantly improve the upper limit on the tensor-to-scalar ratio r , with $\sigma(r) < 10^{-3}$. However, if r is large enough, tentative B -mode detections could be reported from the ground or by balloon experiments ahead of this mission. The significance of such a discovery would be such that the detailed characterization of the angular and spectral dependence of the signal, as well as the verification of its isotropy across the sky, both of which are uniquely enabled by a satellite mission, would be required to confirm its primordial origin (cite Decadal Survey).

In this scenario, a probe-class mission will in particular detect and characterize the reionization signal expected at the largest angular scales (multipoles below ~ 10), where observations from other platforms are the most challenging. The contribution from reionization to the Stokes parameter Q for $r = 0.001$ is shown in the left panel of Figure 5. The amplitude of this signal is ~ 10 nK, which requires that any experiment attempting to measure it control large-scale foregrounds and systematics at the unprecedented level of a few nK.

1.3.1 Foregrounds

Data from the *Planck* satellite have significantly improved our understanding of foregrounds in both intensity and polarization. In polarization, the sky is dominated by synchrotron radiation and the emission from interstellar dust. *Planck* has provided us with much improved measurements of

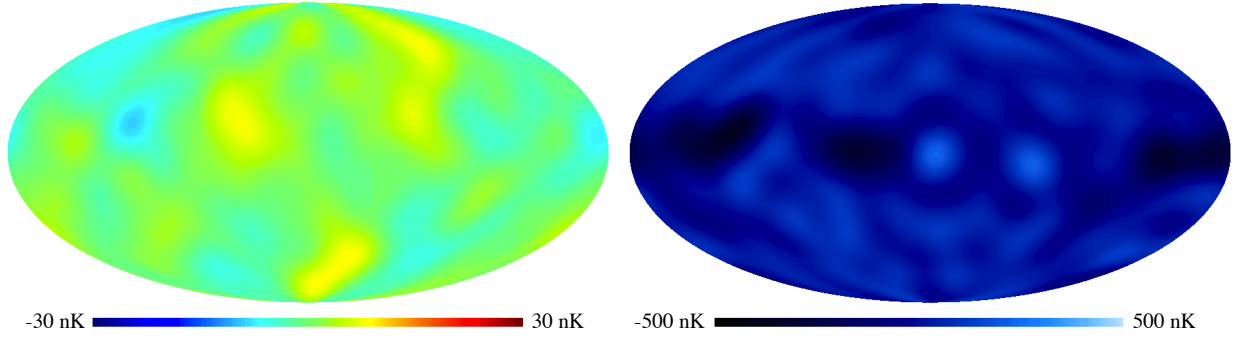


Figure 5: *Left panel:* Contribution to the Stokes Q parameter from inflationary B -modes for $\ell < 12$ and $r = 0.001$. *Right panel:* Noise in the *Planck* 353 GHz map of the Stokes Q parameter for $\ell < 12$ rescaled to 150 GHz assuming the spectral properties of dust.

their amplitude and spectral dependence. The observed frequency spectra of both foregrounds are shown for three sky fractions in the left panel of Figure 6. *Even in the cleanest patches of the sky*, polarized foreground emission is brighter than the sought-after primordial B -mode signal by over an order of magnitude at all frequencies. This statement holds at all angular scales relevant to the search for primordial B -modes, as shown in the right panel of Figure 6.

Perfect knowledge of the foreground components would enable their removal from microwave data, but the sensitivity of the *Planck* measurements limits it at a level insufficient to detect primordial B -modes, even for values of $r \sim 10^{-1}$. The right panel of Figure 5 shows the noise in the *Planck* 353 GHz map of the Stokes Q parameter at the angular scales relevant for primordial B -mode measurements, and rescaled to 150 GHz assuming the spectral dependence of dust; it is over an order of magnitude larger than the inflationary contribution for $r = 0.001$. A mission aiming to detect primordial B -modes at this level across the sky will therefore not be able to rely on existing data. High signal-to-noise foreground measurements must accompany those at frequencies where the CMB contribution is larger. As discussed below, optimizing the frequency coverage of these measurements will be a key goal of the mission concept study.

While the search for primordial B -modes leads to the strictest constraints on foreground residuals, exquisit control of foregrounds is also necessary for other science objectives enabled by a probe-class mission, including measuring the optical depth to last scattering τ at a level necessary to break its degeneracy with the sum of neutrino masses Σm_ν , probing star formation history with a cosmic-variance limited measurement of the large-scale E -mode polarization of the CMB, and detecting the μ -distortion generated in Λ CDM by the dissipation of small-scale acoustic modes.

One of the key ingredients in the design of a CMB experiment is the frequency coverage required to achieve its science goals. This optimization will be one of the key objectives of the proposed study. We will leverage the foreground information provided by *Planck* as well as ground-based and balloon-borne experiments, with a particular focus on propagating measurement uncertainties through to forecasts. In particular, we plan a careful investigation of the effect on the measurements of r and τ of the presence of foreground residuals in the CMB maps (after foreground separation and/or cleaning) including, for example, the properties of the polarized thermal dust emission, specifically the spatial variation of its spectral index hinted at by the observed decorrelation of the dust between 217 GHz and 353GHz *Planck* channels ([? ? ? ?]), the break-

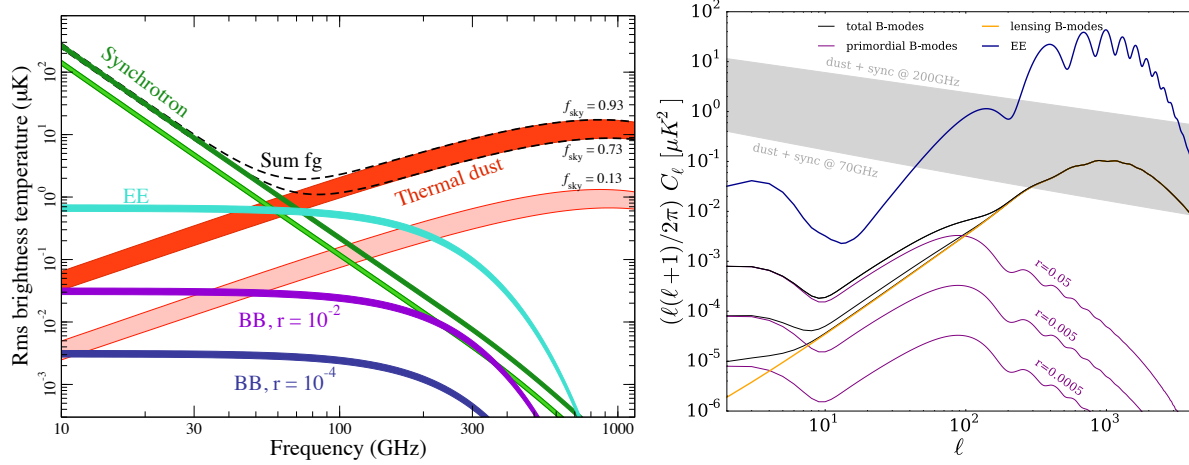


Figure 6: *Left panel:* Brightness temperature as a function of frequency for the CMB, synchrotron emission (green), and dust emission (red). The darker (respectively, lighter) bands show brightness temperatures for sky fractions between 73% and 93% (respectively, for the cleanest 13% of the sky, with the width indicating the uncertainty). *Right panel:* Angular power spectrum for CMB E - and B -modes with $r = 0.0005$, $r = 0.005$, and $r = 0.05$, as well as for foreground emission between 70 and 200 GHz for $f_{\text{sky}} = 75\%$.

down of the modified black body spectrum model, and decorrelation between frequencies. These aspects will be explored with the help of physically motivated models of the foregrounds ([? ?]) informed by existing data and simulations based on these, using either existing simulation tools and/or implementing new simulators when required.

The optimization of frequency channels will be conducted using both traditional (Fisher codes both spectra and map based) and novel techniques currently in development (such as direct Bayesian MCMC inference of cosmological parameters in the presence of foregrounds, (extension of the method presented in [?])). Realistic simulations (including time domain based) are essential to fully assess the performance of a given instrument design/concept in view of both foreground residuals and the presence of systematics. We plan to generate these simulations, process them as we would do the real data, specifically applying some of the current component separation methods to clean the frequency maps from foreground emission (akin to *Planck* collaboration procedures [?]) and propagate to parameter estimation, assessing the impact of all contaminating effects on the accuracy and potential biases of the parameters estimated with particular emphasis on r and τ .

1.3.2 Systematic Errors

Advances in detector technology since the formulation of *Planck* and *WMAP* will enable huge gains in raw sensitivity for a CMB probe. To fully take advantage of this sensitivity, systematic errors must be controlled to detect polarization signals at nano-Kelvin levels. The proposed study will invest heavily in designing an instrument, test plan, and observation strategy to address systematic errors, gathering decades of experience of ground-, balloon-, and space-based CMB polarimetry. The latest experience with *Planck* points to the following systematic error categories likely to be important for a future space mission [?]: 1. Intensity-to-polarization leakage, 2. stability, and 3. straylight.

Leakage The CMB anisotropy signal is a factor of 1000 larger than the strongest possible inflationary B -mode signal (see for example Fig. 1). Therefore instrumental effects that can leak

even a small fraction of an intensity fluctuation into spurious polarization must understood and controlled. The main effects are differences between gains of detectors sensitive to two orthogonal polarization states, their frequency bandpass mismatch, their differential pointing on the sky, and their differential antenna patterns. These differential effects need to be controlled, through instrument design, characterization, or data analysis to 1 part in 10^4 to give a negligible contribution for $\sigma(r) < 0.001$. This level of control represents a factor of 100 improvement on *Planck*'s performance [?].

A second order complication of unmatched bandpasses is unmatched far sidelobe contamination, leading to a spurious polarized component from bright unpolarized signals far from the main lobe.

These systematics are likely to drive the instrumental requirements on the optical system as well as the uniformity of the bandpass of each polarimeter. Calibration requirements will also be set by limiting these systematics: particularly on the knowledge of the polarization parameters (such as cross-polar leakage and the angle of polarization sensitivity), as well as measurement of the beam shape (in general a function of the SED of the observed source). These systematic effects can potentially be mitigated by modulation of the sky signal in such a way that allows complete reconstruction of the polarized sky signal using each photometer, for example, using a half-wave plate.

Stability. Given the need to avoid light from the Sun, Earth, and Moon, the full reconstruction of the polarized sky will necessarily involve combination of measurements made at times separated by months, requiring stability of the response of the instrument on corresponding time scales. This systematic error puts requirements on control of thermal drifts of spacecraft temperatures, to mitigate thermal emissivity changes and thermoelastic deformation of telescope structures. The cryogenic operating temperatures of detectors or reference calibration loads must be controlled adequately as well. Careful design of the scan strategy can shorten the time scales needed for stringent stability, for example *Planck*'s scan strategy traced out great circles which overlapped on 1 minute timescales, giving a shorter effective time scale for stability requirements.

Additionally, the space radiation environment is modulated by the solar activity and can introduce drifts in the cryogenic thermal environment as well as introducing correlated transients in detectors and readout electronics. The design of the instrument must account this environment, which following *Planck* is much better understood.

Straylight. The brightest cm-wave and mm-wave sources in the sky (such as the Sun, Moon, planets, and Galactic center) passing into the far sidelobes of the telescope (defined as the response of a detector from a source more than a few degrees from the optical axis) in a sky-synchronous way can create a spurious polarization signal. The far sidelobe response can be reduced by the optical design and baffling, but will always be present at a non-trivial level. The *Planck* experience is instructive here as well. The detailed GRASP model of the telescope, convolved with the sky model, predicted sidelobe contamination at a visible (10's of microK) level in the 30 GHz maps, which was observed in difference maps. As a result the LFI maps have had an estimate of the sidelobe contamination removed from the timelines as part of the mapmaking process. The more stringent requirements for CMB-probe will necessitate at least this level of mitigation. A major limitation to the analysis of far sidelobe contamination in the *Planck* data has been the lack of bright enough on-orbit sources to validate the GRASP simulation as adjusted by optical and bandpass parameters estimated on-orbit. Finding a way to better validate the FSL model on-orbit for CMB-probe may be critical to successfully removing FSL contamination.

1.4 Current and Forthcoming Efforts and the CMB Probe

The remarkable scientific yield resulting from past CMB observations has motivated significant investments in current and future experiments which are designed to realize the full potential of this unique probe of fundamental physics. These ground-based and balloon-borne experiments are designed to exploit the comparative advantages of the sub-orbital platforms over an orbital mission, while providing the design heritage and experience necessary to maximize the probability of success of an orbital mission.

For the ground-based efforts, these include combinations of *i*) provision for large primary apertures and therefore high angular resolution, *ii*) extremely long observation times, *iii*) flexibility to rapidly deploy new technologies, and *iv*) allowance for detector formats that are relatively unconstrained by mass and power limitations. In aggregate, these enable extremely low noise measurements of small scale anisotropies with high redundancy over large areas of the sky.

The balloon-borne missions *i*) extend the frequency reach of the ground based telescopes, *ii*) enable high fidelity measurements on larger angular scales than can be probed from the ground, and *iii*) grant inexpensive access to a space-like environment, providing heritage for future space missions as well as experience in dealing with the analysis of data that are representative of a space mission.

In this way, the sub-orbital programs complement and multiply the scientific return of the proposed orbital mission, while reinforcing its technical preparedness. A robust program of sub-orbital experimentation has proven a vital component in the success of all three generations of previous CMB orbital missions – COBE, WMAP and *Planck*. Building on this heritage, the current (Stage-3) and planned (Stage-4) sub-orbital experiments are well poised to play a similar role for the CMB Probe, which will provide definitive measurements of the full sky from the largest angular scales to the $5'$ scale of the beam.

Ground based experiments are already approaching the level of sensitivity of the CMB Probe over limited portions of the sky ($< 1\%$ of the full sky), and a limited range in frequency. Balloon-borne experiments and ground based telescopes at mid-latitudes are now beginning to extend these measurements to significant fractions of the full sky. Currently funded balloon borne experiments will add to this sensitive data at frequencies above 200 GHz which will help characterize Galactic dust, while ground based experiments in Chile will add critical information at lower frequencies to constrain synchrotron emission. The Stage-4 experiments will extend these measurements to much larger areas, and to angular scales smaller than $5'$, with benefits to the CMB Probe as described in Section 1.2.

The CMB Probe will add to these complete sky coverage, fidelity to the largest angular scales, comprehensive frequency coverage and exquisite control of systematic effects. As evidenced by the experience of Bicep and *Planck*, the joint analyses are becoming increasingly important to fully exploit the scientific value of CMB data sets. As part of this mission study, we will organize a workshop to organize this effort, and investigate the ways in which the ground and sub-orbital balloon programs can best complement the CMB probe.

1.5 State of Technologies

2 pages. Discuss the technologies, their TRL, and what will be studied

A fourth generation CMB satellite targeting a map sensitivity of $\sim 1\mu k - \text{arcmin}$ will require, extremely sensitive detector arrays, tight control over systematics, and ability to reject polarized foregrounds as is described in Section 1.2. Given the frequency dependence of synchrotron and dust foregrounds, this last requirement translates into the need for a large number of spectral bands

covering the approximate frequency range from ~ 30 GHz to ~ 800 GHz. Development of the CMB technologies needed to meet these requirements is actively being pursued by many groups who are also demonstrating these technologies on ground, balloon, and satellite platforms. We describe the status and needs in the areas of telescopes, optics, detector coupling, detectors, and readout.

Telescopes: Carbon Fiber Reinforced Polymer (CFRP) mirrors are at TRL 9 as they have flown on the Planck satellite. Their 1.9×1.5 m mirror weighted only 28 lbs and met all surface quality requirements. However, small deformations in the mirror caused by its structural supports had a measurable impact to the beam far-sidelobes that was not captured by preflight measurements or the corresponding beam modeling. Future CMB satellites will require improved pre-flight characterization of *polarized beam* at operating temperature augmented by improved simulation tools to meet even more systematics requirements. Current ground and balloon born optical designs achieve large field of views (FOVs) with reflective and refractive designs; related designs and their implementation should be studied in the context of a satellite mission as the sensitivity requirements lead to the need to maximize the size of the FOV while fitting within the tight mass and size constraints imposed by a space mission. Given the heritage of past satellite missions it will be possible to develop a telescope design that meets the requirements for a future mission and uses high TRL components.

Optical Coupling: The need for sensitivity drives the push for high efficiency optics; wide bandwidth to complement multichroic detector; infrared filters to maximize cryogenic performance; and polarization modulators to suppress $1/f$ noise and mitigate instrument systematics. The CMB field has made tremendous progress recently by drawing on advances in materials, processing techniques, and developments in electrical engineering including meta-material research. Single crystals such as silicon and sapphire are attractive since they offer extremely low dielectric losses and high indices of refraction to better manipulate light. New coating techniques have been developed for silicon and sapphire that span 2:1 bandwidth (TRL 5+ for silicon) and can realize up to 5:1 bandwidth. EBEX deployed broadband cryogenic polarization modulator with a superconducting bearing that covered 150 GHz band to 410 GHz band raising the modulators to TRL 5+ for space. Meta-material metal-mesh optical filters were deployed with the Planck satellite and they are extensively used by ground based and balloon experiments making these TRL6 optical elements. It is necessary to develop a plan for a satellite mission that will cover ~ 30 GHz to ~ 800 GHz. Two configurations could be considered: multiple optical paths with $< 3 : 1$ bandwidth and a potentially simpler design with only two optical paths with $\sim 5 : 1$ bandwidth. These studies include evaluating the design tradeoffs inherent to these approaches, developing the new coatings needed, and evaluating the promise of hybrid approaches where filters and lenses are implemented in the same optical elements. In addition, the cryogenic rotation mechanism should be demonstrated at the robustness (eg lifetime) needed for a satellite mission.

Detector Coupling: The focal-plane feed determines the shape and polarization properties of the pixel beams and therefore plays a strong role in controlling systematic errors. The feed design also can determine the total bandwidth and number of photometric bands of each pixel which is important for the efficient use of a telescope's focal plane area. CMB experiments developed broadband multi-chroic *detector* to increase optical throughput of a focal plane. Broadband feed captures sig-

nal over wide frequency range. Then on-chip superconducting filter partitions signal into multiple frequency bands prior to detection. Broadband detectors were realized with spline profiled horn and lenslet coupled antenna. Broadband horn detector deployed a pixel that covers 2.3:1 bandwidth with on going development for extending bandwidth to 6:1. Broadband lenslet coupled antenna will deploy 3:1 bandwidth detector this year. Lenslet coupled antenna demonstrated 5:1 bandwidth in laboratory. RF-techniques to partition broadband signals into multiple band are mature. For a future CMB polarization satellite mission, broadband feed should be demonstrated at high frequency where alignment and line width for micro-fabrication becomes challenging. Detectors for CMB satellite mission were hand picked one by one for optimal performance. Next generation of detector array will be fabricated on a silicon wafer. Micro-fabrication process should demonstrate high yield and uniformity across a wafer that can meet tight requirement of satellite mission. Also detector test need to able to characterize detector beyond the level of systematic required by next generation CMB satellite experiment.

The Planck HFI deployed Neutron Transmutation Doped Germanium high-resistance bolometer at 100 milli-Kelvin to achieve photon noise limited detector performance. A Transition Edge Sensor (TES) bolometer uses a steep transition of superconducting metal to improve linearity of the detector. TES bolometers have been deployed on 100 milli-Kelvin and 250 milli-Kelvin platform. TES bolometers have been deployed across ground based and balloon CMB experiments spanning 40 GHz-410 GHz with detectors achieving NEPs of $20\text{-}50\text{ aW}/\sqrt{\text{Hz}}$, nearly background limited at CMB frequencies. TES bolometers deployed at low optical frequencies ($\sim 40\text{ GHz}$) and balloon-borne payloads should realized even lower NEPs of $\sim 10\text{ aW}/\sqrt{\text{Hz}}$. Emerging detector technology for CMB experiment is kinetic-inductance detector (KIDs). The KIDs detector detects signal as change in kinetic inductance. KIDs detectors can be frequency multiplexed easily to $\sim 1,000$ detectors. Recently, on-sky demonstration at 150 GHz and 230 GHz was done with lumped element KID detector. Noise performance of KID detector at low frequency channels ($< 40\text{ GHz}$) need some improvement to be photon-noise limited. Currently there is no CMB polarizatin power spectrum data produced with KID detector. Coupling between RF (100 GHz) signal to micro-wave KID (MKID) detector is in a development stage. Planck detectors experienced unexpectedly high rate of cosmic ray events. Data was successfully cleaned with analysis technique. Study of impact of cosmic rays on a detector is crucial for next CMB satellite mission.

Multiplexed readout is being used by CMB experiments to readout thousands of TES bolometers, and readout multiplexing is built into KID detector architecture. Voltage bias and low impedance of a TES bolometer facilitates multiplexing readout by Superconducting Quantum Interference Device (SQUID). Time domain multiplexing uses a SQUID at milli-Kelvin as a switch to rapidly cycle through bolometers. Highest achieved multiplexing factor is 64 channels. Frequency domain multiplexing uses superconducting resonators to assign bolometers to different frequency channels. Highest achieved multiplexing factor is 68 channels. New readout scheme, such as microwave SQUID readout, is emerging to increase multiplexing factor for TES bolometer. MKID detector architecture has multiple resonators coming off from a transmission line. A resonator is both a detector and multiplexer. MKID demonstrated multiplexing factor that exceeds 1,000 channels. For next generation satellite experiment that will readout over thousands detectors require high multiplexing factor. Multiplexing factor is directly related to readout complexity and power consumption. Also the Planck mission experienced ADC non-linearity, thus extensive characterization of end to end readout architecture should be performed pre-flight.

A future CMB satellite mission offers exciting opportunity for millimeter wave polarization science. Experience from Planck mission will be studied to learn lessons for the future mission.

Development for CMB instrumentation is an active field with many institutions developing new technologies for ground based, balloon, and proposed satellite missions. For a satellite instrumentation, there is a difficult trade off between desire to have high performance instrument and desire to keep cost manageable. Many developments that is going on for ground based and balloon experiment have similar goal as satellite mission that collaborative development across all platform will be beneficial.

1.6 Mission Study, and Management Plan

Shaul is writing this.

References

- [1] J. Bock, A. Aljabri, A. Amblard, D. Baumann, M. Betoule, T. Chui, L. Colombo, A. Cooray, D. Crumb, P. Day, C. Dickinson, D. Dowell, M. Dragovan, S. Golwala, K. Gorski, S. Hanany, W. Holmes, K. Irwin, B. Johnson, B. Keating, C.-L. Kuo, A. Lee, A. Lange, C. Lawrence, S. Meyer, N. Miller, H. Nguyen, E. Pierpaoli, N. Ponthieu, J.-L. Puget, J. Raab, P. Richards, C. Satter, M. Seiffert, M. Shimon, H. Tran, B. Williams, and J. Zmuidzinas. Study of the Experimental Probe of Inflationary Cosmology (EPIC)-Intermediate Mission for NASA's Einstein Inflation Probe. *ArXiv e-prints*, June 2009.
- [2] A. Kogut, D. J. Fixsen, D. T. Chuss, J. Dotson, E. Dwek, M. Halpern, G. F. Hinshaw, S. M. Meyer, S. H. Moseley, M. D. Seiffert, D. N. Spergel, and E. J. Wollack. The Primordial Inflation Explorer (PIXIE): a nulling polarimeter for cosmic microwave background observations. *JCAP*, 7:25–+, July 2011.
- [3] J. C. Mather, E. S. Cheng, D. A. Cottingham, R. E. Eplee, Jr., D. J. Fixsen, T. Hewagama, R. B. Isaacman, K. A. Jensen, S. S. Meyer, P. D. Noerdlinger, S. M. Read, and L. P. Rosen. Measurement of the cosmic microwave background spectrum by the COBE FIRAS instrument. *Ap. J.*, 420:439–444, January 1994.
- [4] D. J. Fixsen, E. S. Cheng, J. M. Gales, J. C. Mather, R. A. Shafer, and E. L. Wright. The Cosmic Microwave Background Spectrum from the Full COBE FIRAS Data Set. *Ap. J.*, 473:576–+, December 1996.
- [5] Y. B. Zeldovich and R. A. Sunyaev. The Interaction of Matter and Radiation in a Hot-Model Universe. *ApSS*, 4:301–316, July 1969.
- [6] R. A. Sunyaev and Y. B. Zeldovich. The interaction of matter and radiation in the hot model of the Universe, II. *ApSS*, 7:20–30, April 1970.
- [7] R. Keisler, C. L. Reichardt, K. A. Aird, B. A. Benson, L. E. Bleem, J. E. Carlstrom, C. L. Chang, H. M. Cho, T. M. Crawford, A. T. Crites, T. de Haan, M. A. Dobbs, J. Dudley, and E. M. George. A Measurement of the Damping Tail of the Cosmic Microwave Background Power Spectrum with the South Pole Telescope. *Ap. J.*, 743:28, December 2011.
- [8] <http://bolo.berkeley.edu/polarbear/>.
- [9] A. H. Guth. Inflationary universe: A possible solution to the horizon and flatness problems. *Phys. Rev. D.*, 23:347–356, January 1981.
- [10] A. D. Linde. A New Inflationary Universe Scenario: A Possible Solution of the Horizon, Flatness, Homogeneity, Isotropy and Primordial Monopole Problems. *Phys. Lett.*, B108:389–393, 1982.
- [11] A. Albrecht and P. J. Steinhardt. Cosmology for grand unified theories with radiatively induced symmetry breaking. *Phys. Rev. Lett.*, 48:1220–1223, 1982.
- [12] K. Sato. First-order phase transition of a vacuum and the expansion of the Universe. *MNRAS*, 195:467–479, May 1981.

- [13] E. W. Kolb and M. S. Turner. *The Early Universe*. Addison-Wesley, Redwood City, CA, 2nd. edition, 1994.
- [14] M. Kamionkowski, A. Kosowsky, and A. Stebbins. A Probe of Primordial Gravity Waves and Vorticity. *Phys. Rev. Lett.*, 78:2058–2061, March 1997. astro-ph/9609132.
- [15] M. Zaldarriaga and U. Seljak. All-sky analysis of polarization in the microwave background. *Phys. Rev. D.*, 55:1830–1840, 1997.
- [16] Hayden Lee, S. C. Su, and Daniel Baumann. The Superhorizon Test of Future B-mode Experiments. *JCAP*, 1502(02):036, 2015.
- [17] Committee for a Decadal Survey of Astronomy and Astrophysics. *New Worlds, New Horizons in Astronomy and Astrophysics*. National Academy Press, 2010.
- [18] P. A. R. Ade et al. Improved Constraints on Cosmology and Foregrounds from BICEP2 and Keck Array Cosmic Microwave Background Data with Inclusion of 95 GHz Band. *Phys. Rev. Lett.*, 116:031302, 2016.
- [19] Renata Kallosh and Andrei Linde. Universality Class in Conformal Inflation. *JCAP*, 1307:002, 2013.
- [20] David H. Lyth. What would we learn by detecting a gravitational wave signal in the cosmic microwave background anisotropy? *Phys.Rev.Lett.*, 78:1861–1863, 1997.
- [21] Tom Banks, Michael Dine, Patrick J. Fox, and Elie Gorbatov. On the possibility of large axion decay constants. *JCAP*, 0306:001, 2003.
- [22] Daniel Baumann and Liam McAllister. *Inflation and String Theory*. Cambridge University Press, 2015.
- [23] Jon Brown, William Cottrell, Gary Shiu, and Pablo Soler. Fencing in the Swampland: Quantum Gravity Constraints on Large Field Inflation. *JHEP*, 10:023, 2015.
- [24] Tom Rudelius. Constraints on Axion Inflation from the Weak Gravity Conjecture. *JCAP*, 1509(09):020, 2015.
- [25] Eva Silverstein and Alexander Westphal. Monodromy in the CMB: Gravity Waves and String Inflation. *Phys.Rev.*, D78:106003, 2008.
- [26] Nemanja Kaloper and Lorenzo Sorbo. A Natural Framework for Chaotic Inflation. *Phys. Rev. Lett.*, 102:121301, 2009.
- [27] Fernando Marchesano, Gary Shiu, and Angel M. Uranga. F-term Axion Monodromy Inflation. *JHEP*, 09:184, 2014.
- [28] Ralph Blumenhagen, Cesar Damian, Anamaria Font, Daniela Herschmann, and Rui Sun. The Flux-Scaling Scenario: De Sitter Uplift and Axion Inflation. 2015.
- [29] Justin Khoury, Burt A. Ovrut, Nathan Seiberg, Paul J. Steinhardt, and Neil Turok. From big crunch to big bang. *Phys. Rev.*, D65:086007, 2002.

- [30] Robert H. Brandenberger. The Matter Bounce Alternative to Inflationary Cosmology. 2012.
- [31] Anna Ijjas and Paul J. Steinhardt. Implications of Planck2015 for inflationary, ekpyrotic and anamorphic bouncing cosmologies. *Class. Quant. Grav.*, 33(4):044001, 2016.
- [32] Ryo Namba, Marco Peloso, Maresuke Shiraishi, Lorenzo Sorbo, and Caner Unal. Scale-dependent gravitational waves from a rolling axion. *JCAP*, 1601(01):041, 2016.
- [33] Marco Peloso, Lorenzo Sorbo, and Caner Unal. Rolling axions during inflation: perturbativity and signatures. 2016.
- [34] Cora Dvorkin, Hiranya V. Peiris, and Wayne Hu. Testable polarization predictions for models of CMB isotropy anomalies. *Phys. Rev.*, D77:063008, 2008.
- [35] R. A. Sunyaev and Y. B. Zeldovich. Small scale entropy and adiabatic density perturbations - Antimatter in the Universe. *ApSS*, 9:368–382, December 1970.
- [36] R. A. Daly. Spectral distortions of the microwave background radiation resulting from the damping of pressure waves. *Ap. J.*, 371:14–28, April 1991.
- [37] W. Hu, D. Scott, and J. Silk. Power spectrum constraints from spectral distortions in the cosmic microwave background. *Ap. J. Lett.*, 430:L5–L8, July 1994.
- [38] J. Chluba, R. Khatri, and R. A. Sunyaev. CMB at 2 x 2 order: the dissipation of primordial acoustic waves and the observable part of the associated energy release. *MNRAS*, 425:1129–1169, September 2012.
- [39] J. Chluba. Which spectral distortions does Λ CDM actually predict? *MNRAS*, 460:227–239, July 2016.
- [40] R. A. Sunyaev and J. Chluba. Signals from the epoch of cosmological recombination (Karl Schwarzschild Award Lecture 2008). *Astronomische Nachrichten*, 330:657–+, 2009.
- [41] J. Chluba and Y. Ali-Haïmoud. COSMOSPEC: fast and detailed computation of the cosmological recombination radiation from hydrogen and helium. *MNRAS*, 456:3494–3508, March 2016.
- [42] G. Steigman. Cosmology confronts particle physics. *Annual Review of Nuclear and Particle Science*, 29:313–338, 1979.
- [43] M. Bolz, A. Brandenburg, and W. Buchmuller. Thermal production of gravitinos. *Nucl. Phys.*, B606:518–544, 2001. [Erratum: *Nucl. Phys.*B790,336(2008)].
- [44] Christopher Brust, David E. Kaplan, and Matthew T. Walters. New Light Species and the CMB. *JHEP*, 12:058, 2013.
- [45] Daniel Baumann, Daniel Green, and Benjamin Wallisch. A New Target for Cosmic Axion Searches. *Phys. Rev. Lett.*, 117(17):171301, 2016.
- [46] Daniel Green, Joel Meyers, and Alexander van Engelen. CMB Delensing Beyond the B Modes. 2016.

- [47] S. Sarkar and A. M. Cooper. Cosmological and experimental constraints on the tau neutrino. *Physics Letters B*, 148:347–354, November 1984.
- [48] M. Kawasaki and K. Sato. The effect of radiative decay of massive particles on the spectrum of the microwave background radiation. *Physics Letters B*, 169:280–284, March 1986.
- [49] W. Hu and J. Silk. Thermalization constraints and spectral distortions for massive unstable relic particles. *Physical Review Letters*, 70:2661–2664, May 1993.
- [50] J. Chluba and R. A. Sunyaev. The evolution of CMB spectral distortions in the early Universe. *MNRAS*, 419:1294–1314, January 2012.
- [51] J. Chluba. Distinguishing different scenarios of early energy release with spectral distortions of the cosmic microwave background. *MNRAS*, 436:2232–2243, December 2013.
- [52] J. Chluba and D. Jeong. Teasing bits of information out of the CMB energy spectrum. *MNRAS*, 438:2065–2082, March 2014.
- [53] M. Kawasaki, K. Kohri, and T. Moroi. Big-bang nucleosynthesis and hadronic decay of long-lived massive particles. *Phys. Rev. D.*, 71(8):083502, April 2005.
- [54] K. Jedamzik. Big bang nucleosynthesis constraints on hadronically and electromagnetically decaying relic neutral particles. *Phys. Rev. D.*, 74(10):103509, November 2006.
- [55] P. J. E. Peebles, S. Seager, and W. Hu. Delayed Recombination. *Ap. J. Lett.*, 539:L1–L4, August 2000.
- [56] X. Chen and M. Kamionkowski. Particle decays during the cosmic dark ages. *Phys. Rev. D.*, 70(4):043502–+, August 2004.
- [57] N. Padmanabhan and D. P. Finkbeiner. Detecting dark matter annihilation with CMB polarization: Signatures and experimental prospects. *Phys. Rev. D.*, 72(2):023508–+, July 2005.
- [58] Cora Dvorkin, Kfir Blum, and Marc Kamionkowski. Constraining Dark Matter-Baryon Scattering with Linear Cosmology. *Phys. Rev.*, D89(2):023519, 2014.
- [59] Francis-Yan Cyr-Racine, Roland de Putter, Alvis Raccanelli, and Kris Sigurdson. Constraints on Large-Scale Dark Acoustic Oscillations from Cosmology. *Phys. Rev.*, D89(6):063517, 2014.
- [60] Manuel A. Buen-Abad, Gustavo Marques-Tavares, and Martin Schmaltz. Non-Abelian dark matter and dark radiation. *Phys. Rev.*, D92(2):023531, 2015.
- [61] Julien Lesgourgues, Gustavo Marques-Tavares, and Martin Schmaltz. Evidence for dark matter interactions in cosmological precision data? *JCAP*, 1602(02):037, 2016.
- [62] Y. Ali-Haïmoud, J. Chluba, and M. Kamionkowski. Constraints on Dark Matter Interactions with Standard Model Particles from Cosmic Microwave Background Spectral Distortions. *Physical Review Letters*, 115(7):071304, August 2015.

- [63] R. Essig, A. Manalaysay, J. Mardon, P. Sorensen, and T. Volansky. First Direct Detection Limits on Sub-GeV Dark Matter from XENON10. *Physical Review Letters*, 109(2):021301, July 2012.
- [64] C. Bøhm, J. A. Schewtschenko, R. J. Wilkinson, C. M. Baugh, and S. Pascoli. Using the Milky Way satellites to study interactions between cold dark matter and radiation. *MNRAS*, 445:L31–L35, November 2014.
- [65] K. Jedamzik, V. Katalinić, and A. V. Olinto. Limit on Primordial Small-Scale Magnetic Fields from Cosmic Microwave Background Distortions. *PRL*, 85:700–703, July 2000.
- [66] H. Tashiro, E. Sabancilar, and T. Vachaspati. CMB distortions from superconducting cosmic strings. *Phys. Rev. D.*, 85(10):103522, May 2012.
- [67] A. D. Dolgov and D. Ejlli. Resonant high energy graviton to photon conversion at the post-recombination epoch. *Phys. Rev. D.*, 87(10):104007, May 2013.
- [68] H. Tashiro, J. Silk, and D. J. E. Marsh. Constraints on primordial magnetic fields from CMB distortions in the axiverse. *Phys. Rev. D.*, 88(12):125024, December 2013.
- [69] R. R. Caldwell and N. A. Maksimova. Spectral distortion in a radially inhomogeneous cosmology. *Phys. Rev. D.*, 88(10):103502, November 2013.
- [70] Manoj Kaplinghat, Lloyd Knox, and Yong-Seon Song. Determining neutrino mass from the CMB alone. *Phys. Rev. Lett.*, 91:241301, 2003.
- [71] Michael Levi et al. The DESI Experiment, a whitepaper for Snowmass 2013. 2013.
- [72] J. S. Dunlop. The Cosmic History of Star Formation. *Science*, 333:178, July 2011.
- [73] Planck Collaboration, R. Adam, P. A. R. Ade, N. Aghanim, M. Arnaud, J. Aumont, C. Baccigalupi, A. J. Banday, R. B. Barreiro, J. G. Bartlett, and et al. Planck intermediate results. XXX. The angular power spectrum of polarized dust emission at intermediate and high Galactic latitudes. *ArXiv e-prints*, September 2014.
- [74] Planck Collaboration, P. A. R. Ade, N. Aghanim, C. Armitage-Caplan, M. Arnaud, M. Ashdown, F. Atrio-Barandela, J. Aumont, C. Baccigalupi, A. J. Banday, and et al. Planck 2013 results. XVIII. The gravitational lensing-infrared background correlation. *Astron. Astrophys.*, 571:A18, November 2014.
- [75] P. Madau and M. Dickinson. Cosmic Star-Formation History. *ARA&A*, 52:415–486, August 2014.
- [76] J. C. Hill, N. Battaglia, J. Chluba, S. Ferraro, E. Schaan, and D. N. Spergel. Taking the Universe’s Temperature with Spectral Distortions of the Cosmic Microwave Background. *Physical Review Letters*, 115(26):261301, December 2015.
- [77] Planck Collaboration, P. A. R. Ade, N. Aghanim, C. Armitage-Caplan, M. Arnaud, M. Ashdown, F. Atrio-Barandela, J. Aumont, C. Baccigalupi, A. J. Banday, and et al. Planck 2013 results. XX. Cosmology from Sunyaev-Zeldovich cluster counts. *Astron. Astrophys.*, 571:A20, November 2014.

- [78] S. Y. Sazonov and R. A. Sunyaev. Cosmic Microwave Background Radiation in the Direction of a Moving Cluster of Galaxies with Hot Gas: Relativistic Corrections. *Ap. J.*, 508:1–5, November 1998.
- [79] N. Itoh, Y. Kohyama, and S. Nozawa. Relativistic corrections to the sunyaev-zeldovich effect for clusters of galaxies. *Ap. J.*, 502:7, July 1998.
- [80] A. Challinor and A. Lasenby. Relativistic corrections to the sunyaev-zeldovich effect. *Ap. J.*, 499:1, May 1998.
- [81] J. A. Rubiño-Martín, C. Hernández-Monteagudo, and R. A. Sunyaev. The imprint of cosmological hydrogen recombination lines on the power spectrum of the CMB. *Astron. Astrophys.*, 438:461–473, August 2005.
- [82] C. Hernández-Monteagudo, J. A. Rubiño-Martín, and R. A. Sunyaev. On the influence of resonant scattering on cosmic microwave background polarization anisotropies. *MNRAS*, 380:1656–1668, October 2007.
- [83] A. Lewis. Rayleigh scattering: blue sky thinking for future CMB observations. *JCAP*, 8:053, August 2013.
- [84] K. Basu, C. Hernández-Monteagudo, and R. A. Sunyaev. CMB observations and the production of chemical elements at the end of the dark ages. *Astron. Astrophys.*, 416:447–466, March 2004.
- [85] D. R. G. Schleicher, D. Galli, F. Palla, M. Camenzind, R. S. Klessen, M. Bartelmann, and S. C. O. Glover. Effects of primordial chemistry on the cosmic microwave background. *Astron. Astrophys.*, 490:521–535, November 2008.

2 Curriculum Vitae

3 Summary of Work Effort

4 Current and Pending Support

5 Letters of Support

6 Budget Details - Narrative

6.1 Team, and Work Effort

6.1.1 Funded Team Members

6.1.2 Non-Funded Team Members

6.2 Costing Principles

- **Summer Salaries:**
 - **Workshop:**

6.3 University of Minnesota Budget

6.3.1 Direct Labor

6.3.2 Supplies

6.3.3 Travel

6.3.4 Other Direct Costs

Publications and Teleconferencing

Other Subcontracts

6.3.5 Facilities and Administrative Costs

7 Budget Sheets

ACS attitude control system

ADC analog-to-digital converters

ADS attitude determination software

AHWP achromatic half-wave plate

AMC Advanced Motion Controls

ARC anti-reflection coatings

ATA advanced technology attachment

BRC bolometer readout crates

BLAST Balloon-borne Large-Aperture Submillimeter Telescope

CANbus controller area network bus

CIB cosmic infrared background

CMB cosmic microwave background

CMM coordinate measurement machine

CSBF Columbia Scientific Balloon Facility

CCD charge coupled device

DAC digital-to-analog converters

DASI Degree Angular Scale Interferometer

dGPS differential global positioning system

DfMUX digital frequency domain multiplexer

DLFOV diffraction limited field of view

DSP digital signal processing

EBEX E and B Experiment

EBEX2013 EBEX2013

ELIS EBEX low inductance striplines

ETC EBEX test cryostat

FDM frequency domain multiplexing

FPGA field programmable gate array

FCP flight control program

FOV field of view

FWHM full width half maximum

GPS global positioning system

HDPE high density polyethylene

HIM high index materials

HWP half-wave plate

IA integrated attitude

IP instrumental polarization

JSON JavaScript Object Notation

LDB long duration balloon

LED light emitting diode

LCS liquid cooling system

LC inductor and capacitor

LZH Lazer Zentrum Hannover

MCP multi-color pixel

MSM millimeter and sub-millimeter

MLR multilayer reflective

MAXIMA Millimeter Anisotropy eXperiment IMaging Array

NASA National Aeronautics and Space Administration

NDF neutral density filter

PCB printed circuit board

PE polyethylene

PME polarization modulation efficiency

PSF point spread function

PV pressure vessel

PWM pulse width modulation

RMS root mean square

SLR single layer reflective

SMB superconducting magnetic bearing

SQUID superconducting quantum interference device

SQL structured query language

STARS star tracking attitude reconstruction software

SWS sub-wavelength structures

TES transition edge sensor

TDRSS tracking and data relay satellites

TM transformation matrix

UHMWPE ultra high molecular weight polyethylene

UMN University of Minnesota